Polymer Vol. 39 No. 18, pp. 4335–4342, 1998

0032-3861/98/$19.00+0.00

PII: S0032-3861(97)10030-1

Crystallisation and phase behaviour of poly(butylene terephthalate)/polyarylate blends

Jyongsik Jang* and Jongseob Won
Department of Chemical Technology, Seoul National University, San 56-1, Shinlimdong Kwanakgu, Seoul, South Korea
(Received 13 June 1997; revised 4 August 1997; accepted 11 August 1997)

Crystallisation behaviours of poly(butylene terephthalate) (PBT) homopolymer and PBT in PBT/polyarylate (PAr) blend have been studied using *FT*-i.r. spectrometry. In addition, the phase behaviour of the PBT/PAr blend has been investigated using a dynamic mechanical analyser. Several conformational sensitive bands in PBT were investigated using *FT*-i.r. spectra. The peak of carbonyl stretch mode in PBT shifted to a lower wavenumber and some of the intensities of methylene rocking modes or bending modes increased as crystallisation of PBT proceeded. PAr reduced the crystallisation rate of PBT in PBT/PAr blend. In dynamic mechanical thermal analysis, PBT and PAr were completely miscible in amorphous state, irrespective of the composition of the blend. Crystallisation-induced amorphous phase separation of PBT/PAr blend was detected. Single T_g was observed in all compositions in amorphous state. Different phase separation behaviour was observed in PBT- and PAr-rich blends.

(Keywords: poly(butylene terephthalate); polyarylate; crystallisation)

INTRODUCTION

Poly(butylene terephthalate) (PBT)/polyarylate (PAr) blend, due to its miscibility, crystallisability and phase behaviour, has been widely studied in recent years[1–6]. PBT is a semicrystalline polymer. PBT crystallises very rapidly because the glycol residue in PBT is relatively flexible. The crystal structure of PBT is determined by its conformation of glycol residue and very sensitive to external stress[7–9]. It is possible to investigate a number of conformationally sensitive bands with Fourier-transform infrared spectrometry[10–13]. The most sensitive bands of glycol residue in PBT are found in the methylene rocking region, and the C–H bending modes also exhibit good sensitivity in infrared spectroscopy. Recent fast scan time-resolved Fourier transform infrared work has permitted the characterisation of transition of chain conformation in polymers on much smaller time scale than has been possible with either conventional infrared, Raman, or X-ray diffraction.

PBT/PAr blend is known as one of the completely miscible semicrystalline/amorphous blends in the melt or in the amorphous state[1]. Crystallisation kinetics and morphology of semicrystalline polymer in semicrystalline/amorphous blends can be affected by the other component and compositions. In addition, phase separation of amorphous phase induced by crystallisation of semicrystalline polymer was observed in this kind of binary polymer blends[1]. In PBT/PAr blend, this amorphous phase inhomogeneity induced by crystallisation is attributed to the formation of crystal–amorphous interphase or rejection of PAr from the PBT crystal domain[1,14].

In this paper, the crystallisation behaviour of PBT in PBT/PAr blend was investigated using an *FT*-i.r. spectrometer and it was compared with that of PBT homopolymer. Phase behaviour of PBT/PAr blend was also studied with a dynamic mechanical thermal analyser.

* To whom correspondence should be addressed.

EXPERIMENTAL

Materials

PAr (Unitica Co., U-polymer, $T_g = 193°C$, $M_w = 51\,000$) and PBT (Tongyang Co., Skyton 1000-A, $M_w = 30\,000$) were used for this study. The PAr is based on bisphenol-A and isophthalic and terephthalic acid (in the mole ratio of 75/25 isophthalic acid/terephthalic acid). *Figure 1* shows the chemical structures of PBT and PAr. The chain of PBT consists of aromatic rings, carbonyl functional groups and glycol residues. Both polymers were dried in a vacuum oven for 24 h at 80°C before sample preparation in this experiment.

Sample preparation

Blends of PBT/PAr were made by the solution precipitation method of Kimura *et al.*[15]. PBT and PAr were dissolved in 100 ml of 1,1,2,2-tetrachloroethane (TCE)/phenol (40/60) co-solvent and the solution mixture was precipitated in methanol. The coprecipitant was washed with hot methanol several times and dried in a vacuum oven for 3 days at 100°C. The weight fractions of PBT/PAr blends are 8/2, 6/4, 4/6, 2/8. PBT/PAr blend films for *FT*-i.r. spectroscopic analysis were prepared by heat-pressing the solution-precipitated materials at 250°C for 3 min; they were then quenched in an ice-water bath and referred to 'as-prepared'. There was no transesterification reaction between PBT and PAr under these conditions[15–17]. The quenched PBT/PAr blend films were annealed at 210°C at various time intervals. After annealing, the samples were cooled at room temperature and kept in a desiccator until used.

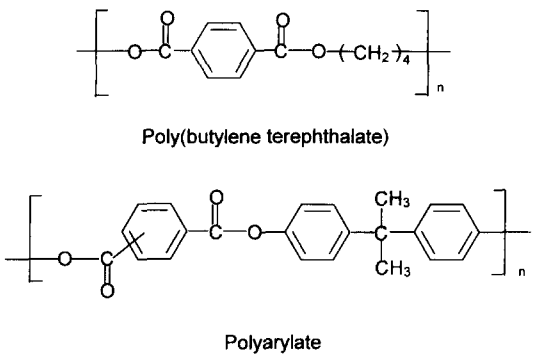

Figure 1 Chemical structures of PBT and PAr

FT-i.r. analysis

All infrared spectra were recorded using a Bomem MB100 Fourier transform infrared spectrometer. Two infrared spectroscopic techniques were used for this study. One was an attenuated total reflectance (ATR) technique for thin film samples (~70 μm thickness) and the other was a transmission technique for sample which was cast on KBr pellet.

The ATR spectra of PBT/PAr blend films were obtained using a germanium (Ge) and zinc selenide (ZnSe) internal reflectance element (IRE). Incident angle was fixed at 45°. Resolution was 2 cm^{-1} and scan number was 100. PBT/PAr blend samples for transmission spectra were prepared according to the following procedure. A solution mixture of PBT and PAr was cast on a KBr pellet. After evaporating solvent at 150°C, the cast blend film was melted at 250°C in a furnace and then quenched to room temperature. An FT-i.r. transmission sample holder was modified. A specially designed thermo-cell fitted with a KBr pellet was utilised to obtain the melt spectra of the PBT/PAr blends. This cell could be heated dynamically with a heat controller.

Thermal analysis

Dynamic mechanical thermal analysis was performed using a rheometrics MK dynamic mechanical analyser (DMA). Data were collected in tensile mode using film

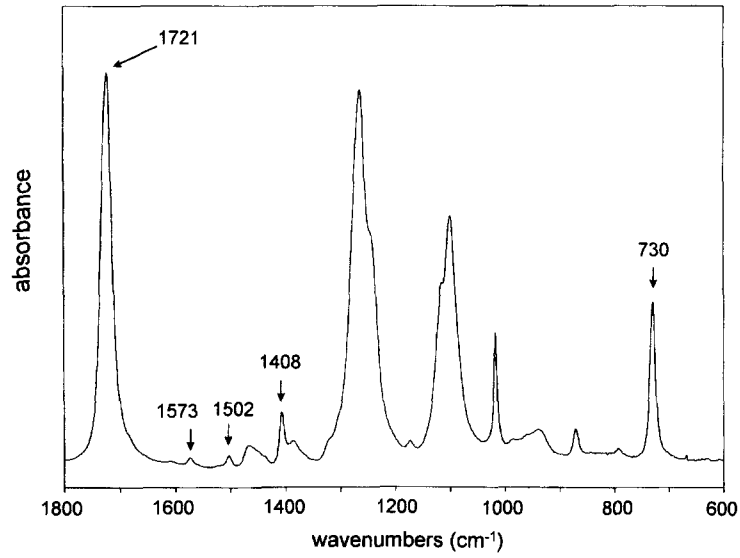

Figure 2 FT-i.r. transmission spectrum of PBT in melt state (at 240°C)

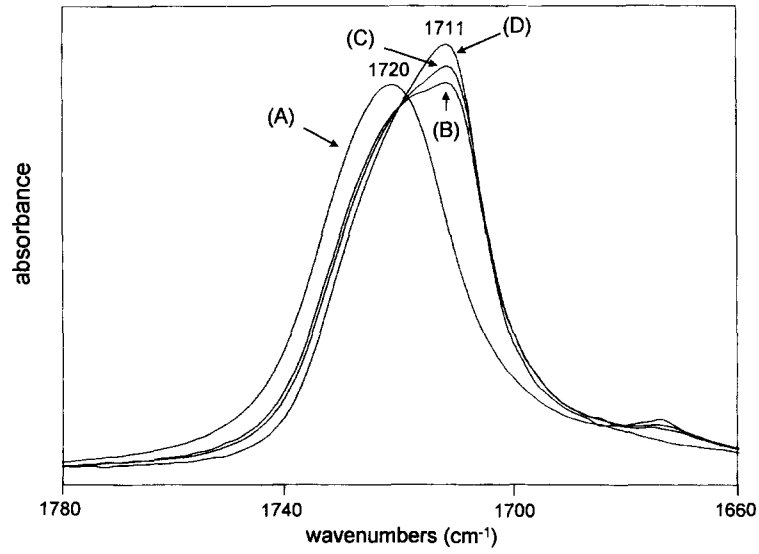

Figure 3 FT-i.r. transmission spectra of PBT in carbonyl region: (*A*) 240; (*B*) 180; (*C*) 148; (*D*) 54°C

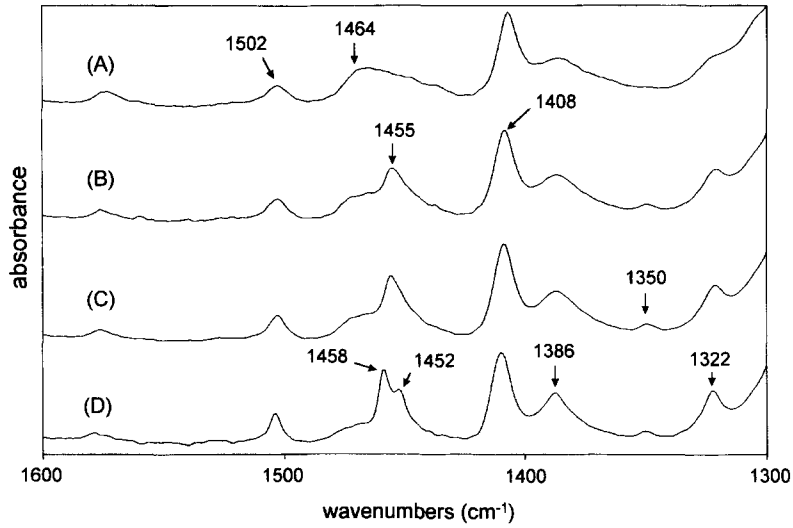

Figure 4 *FT*-i.r. transmission spectra of PBT in methylene bending region: (*A*) 240; (*B*) 180; (*C*) 148; (*D*) 54°C

specimens at a heating rate of 4°C min^{-1} and the frequency was fixed at 1 Hz under nitrogen gas flow. Quenched and annealed blend film samples were analysed using DMA over a temperature range from 40 to 200°C. For dynamic mechanical relaxation, DMA T_g was defined as the position of the maximum of the loss modulus (E'') peak at 1 Hz.

RESULTS AND DISCUSSION

FT-i.r. transmission spectrum of PBT in the melt is shown in *Figure 2*. Since PBT crystallises very rapidly, it was impossible to obtain the spectrum of the perfect amorphous PBT by means of quenching into an ice bath. Therefore, the spectrum of PBT was investigated in the melt state. It is well known that *FT*-i.r. spectra are affected by the physical state and temperature of a polymer[18]. However, the effects of physical state or temperature of samples were relatively small in this case. All peaks of transmission spectra of PBT in the melt state were slightly broader than in the solid state. It can be considered that the spectrum of melt phase PBT is nearly the same as that of perfect amorphous PBT. Aromatic ring stretching in PBT is observed at 1573, 1502, 1408 and 730 cm^{-1}. The peak observed at 1502 cm^{-1} was assigned to the v19a ring mode[19]. Common to all spectra of the model compounds possessing terephthalic residues is a band at 1410 cm^{-1}. For this reason, the peak at 1408 cm^{-1} is assigned to the v19b ring mode[19]. The intensity of this mode seems to slightly increase in the crystal–melt phase transition. The peak at 730 cm^{-1} is attributed to aromatic C–H bond stretching mode, which was observed in other polyesters such as poly(ethylene terephthalate) (PET)[20].

The PBT cast on the KBr pellet, was slowly cooled at a rate of 4°C min^{-1} from 240°C to room temperature. Melt crystallisation of PBT was observed in this condition and transmission spectra were obtained successively. Transmission spectra were focussed on three different regions for investigation of crystallisation behaviour of PBT.

First, the frequency shift and intensity variation of carbonyl stretching mode (1800–1650 cm^{-1}) were studied. *Figure 3* concentrates on C=O stretch vibrations in PBT. In *Figure 3*(*A*), the peak at 1720 cm^{-1} is designated to the carbonyl stretch band of PBT in the perfect amorphous state. As crystallisation of PBT preceded on cooling from 240 to 54°C, the new peak at 1711 cm^{-1} was created and the intensity of this peak was increased gradually in *Figure 3*(*B–D*). Therefore, the peak at 1711 cm^{-1} can be assigned to the C=O stretch band of PBT in crystal phase. The PBT chain forms a lamella or spherulite structure in the crystalline region[21]. The electron density of the C=O bond is lowered due to packing or orientation of the PBT chain. For this reason, the shift of the C=O band can take place to a lower wavenumber.

Secondly, the methylene bending region of the PBT sample is shown in *Figure 4*. A number of conformationally sensitive modes of PBT are also observed in this region. It was reported that PBT has two crystalline phases, α and β forms. By combination of X-ray diffraction and spectroscopic measurements, it has been clearly established that the major effect is a change in the conformation of the glycol residue from the *gauche–trans–gauche* sequence (α form) in the unstressed state to the all-*trans* sequence (β form) under stress[11,12]. The peaks at 1458, 1452, 1350 and 1322 cm^{-1} have been assigned to the CH_2 bending mode in

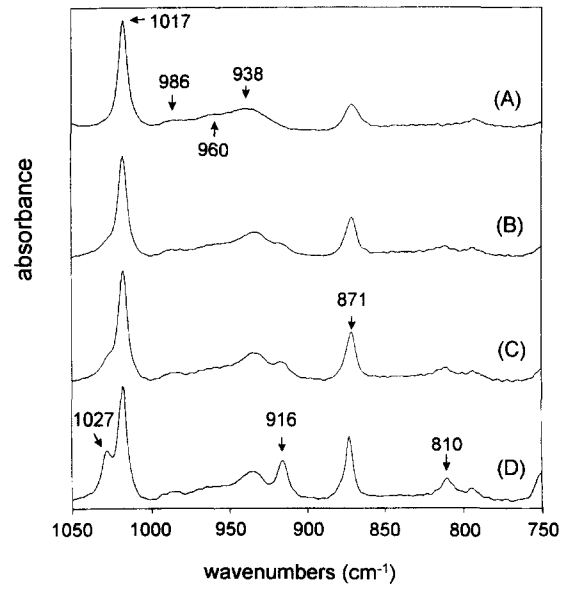

Figure 5 *FT*-i.r. transmission spectra of PBT at methylene rocking region: (*A*) 240; (*B*) 180; (C); 148; (*D*) 54°C

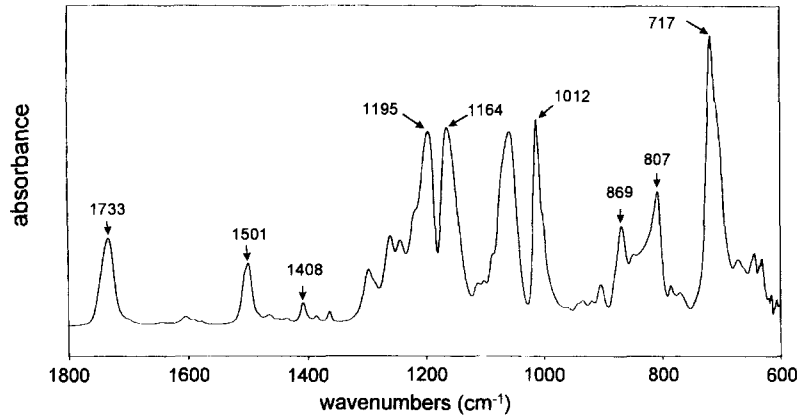

Figure 6 *FT*-i.r. ATR spectrum of polyarylate

the crystalline phase of the α form in PBT. The intensities of these peaks increased on melt crystallisation. It is clear that the band at 1455 cm^{-1} increases and also splits into two bands (1458 and 1452 cm^{-1}). In perfect amorphous or melt state in *Figure 4(A)*, the broadening of the CH_2 bending mode (1480–1420 cm^{-1}) occurs due to coexistence of various conformations of glycol residue in PBT.

The methylene rocking region (1000–850 cm^{-1}) for the same samples in *Figure 3* is shown in *Figure 5*. The peak observed at 1027 cm^{-1} is the C–C stretch mode of glycol residue and the intensity of this peak increased on melt crystallisation of PBT. The bands at 960 and 938 cm^{-1} in *Figure 5(A)* are attributed to the all-*trans* conformation of glycol residues in amorphous PBT [11]. The peak at 916 cm^{-1} shown in *Figure 5(D)* implies that the α phase of PBT contains a type of methylene structure not found in the other phases. This band at 916 cm^{-1} may arise from the non-*trans*:non-*gauche* CH_2–CH_2 structure proposed by Mencik in their X-ray structure determinations[23]. Therefore, the peak at 916 cm^{-1} can be a useful indicator of the α crystal phase of PBT. In addition, the intensities of other CH_2 rocking bands (871 and 810 cm^{-1}) also increase as the crystallinity of the polymer increases.

Polyarylate (PAr) is one of polyesters which are composed of terephthalic acid, isophthalic acid and bisphenol A unit. From the previous publication, PAr can be crystallisable in some solvents[24]. However, there is no thermally induced crystallisation and it can be considered that PAr is a totally amorphous polymer. The *FT*-i.r. ATR spectrum of PAr is shown in *Figure 6*. Several characteristic bands of PAr appeared in this spectrum. For example, the peak at 1733 cm^{-1} is assigned to the C=O stretch mode in the terephthalate unit of PAr. The peaks of the aromatic ring stretch band are observed at 1501 and 1408 cm^{-1}. The aromatic C–H stretch band at 717 cm^{-1} also appeared in this spectrum.

The *FT*-i.r. spectra of quenched PBT/PAr blend films in various compositions are shown in *Figure 7*. The characteristic bands of PBT and PAr are observed in this spectrum, such as the C=O stretch mode, the C–O stretch mode and the aromatic ring stretch mode of PBT or PAr. The intensity of each characteristic peak is approximately proportional to the amount of each component. This result indicates that the blending of PBT/PAr by solution precipitation has been performed successfully under the experimental conditions.

In the PBT/PAr blend, the most sensitive band on crystallisation or annealing was the carbonyl peak of PBT. Heat pressed blend films of PBT/PAr were annealed at 210°C at various time intervals. As PBT crystallises very rapidly, it is considered that 120 min is enough time to crystallisation of PBT. Amorphous and transparent film became opaque in a few minutes. In *Figure 8*, the variation of the carbonyl band in PBT/PAr (4/6) blend are shown as annealing time increases. In PBT/PAr blend, two carbonyl stretch modes are observed. One is due to C=O stretch of PBT, the other is that of PAr. The peak observed at 1714 cm^{-1} is caused by carbonyl stretch band of PBT and 1733 cm^{-1} is carbonyl stretch band of PAr. As shown in *Figure 8*, the intensity of the peak at 1713 cm^{-1} increases and its frequency shifts to lower wavenumber (1707 cm^{-1}) as annealing time increases. Judging from these spectra, the crystallisation of PBT in blend nearly completed within 10 min and new carbonyl stretch mode at lower wavenumber is created by annealing. It is certain that new C=O band is attributed to crystal phase of PBT.

Crystal and amorphous phases coexist in PBT/PAr blend films, as perfect crystallisation of PBT is impossible in the annealing process. These two phases of PBT affect the

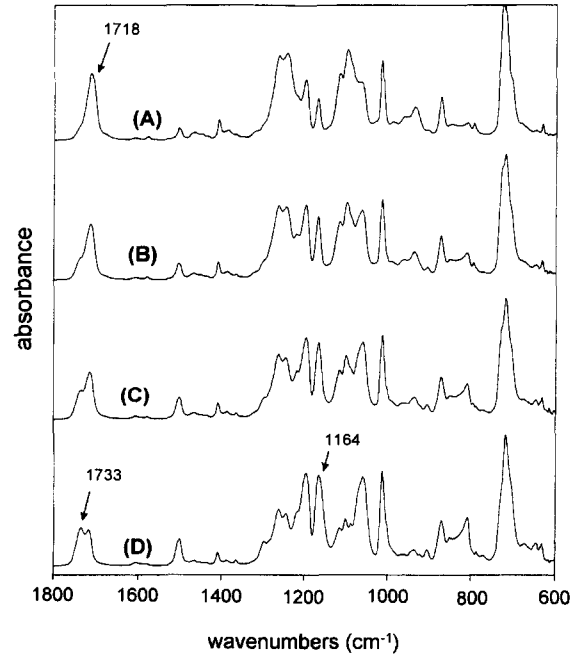

Figure 7 *FT*-i.r. ATR spectra of PBT/PAr blends ('as-prepared'): (*A*) PBT/PAr (8/2); (*B*) 6/4; (*C*) 4/6; (*D*) 2/8

infrared spectrum and bring out the asymmetry and irregular shape of the spectrum. This problem can be solved by mathematical and numerical deconvolution and curve-fitting methods. It was assumed that the carbonyl stretch band at lower wavenumber was due to the crystalline phase of PBT, and one at higher wavenumber was due to the amorphous phase of PBT. The crystallinity of PBT increased with increasing the annealing time. The relative area of the crystalline C=O stretching mode to the amorphous C=O stretching mode of PBT in the infrared spectrum also increased as the annealing time increased. The peak areas with various annealing times were calculated. Calculated results are depicted in *Figure 9*. Judging from this figure, 'as-prepared' sample also contains a slight crystalline phase of PBT. The crystallisation of PBT in blend was nearly finished within 10 min.

Generally, amorphous polymers in semicrystalline/amorphous blends affect the crystallisation of semicrystalline component in three ways[25]. The increment of crystallisation rate or the reduction of crystallisation rate of semicrystalline polymers in amorphous/semicrystalline polymer blends was reported, and sometimes amorphous polymer had no influence on the crystallisation rate of semicrystalline polymer. In the case of PBT/PAr blend, PAr reduced the crystallisation rate of PBT. The carbonyl stretch band variation is shown in *Figure 10* with the same annealing time (3 min) and several composition ratios of blends. As the content of PAr in PBT/PAr blends increased, the crystallinity of PBT in blends decreased. The extent of PBT crystallisation was approximately proportional to the shift width of the carbonyl stretch band of PBT. Therefore, it can be concluded that PAr in a PBT/PAr blend disturbs the crystallisation of PBT, and it depends on the content of PAr in the PBT/PAr blends. The methylene bending region of PBT/PAr (4/6) blends is shown in *Figure 11*. As previously described, the peak observed at 1502 cm^{-1} is assigned to aromatic ring stretch mode in PBT and PAr, this peak has been used as the internal reference peak in all ATR spectra

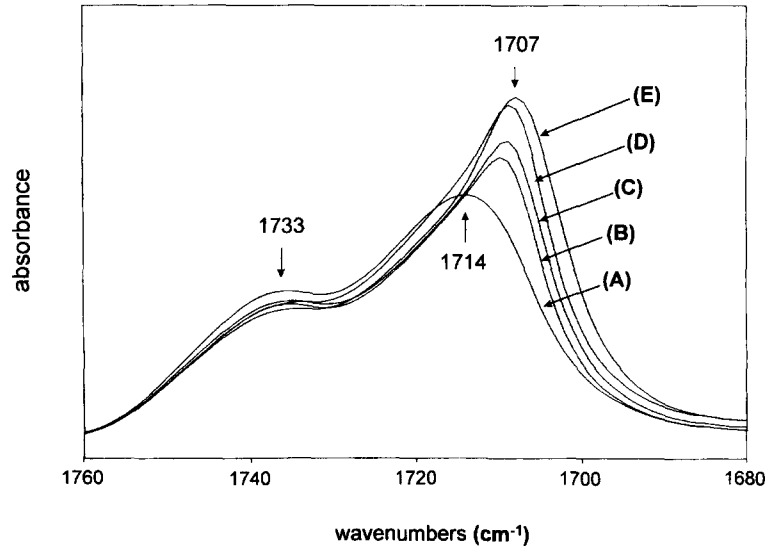

Figure 8 FT-i.r. ATR spectra of PBT/PAr (4/6) blend in carbonyl region annealing time: (*A*) 0; (*B*) 2; (*C*) 3; (*D*) 10; (*E*) 120 min

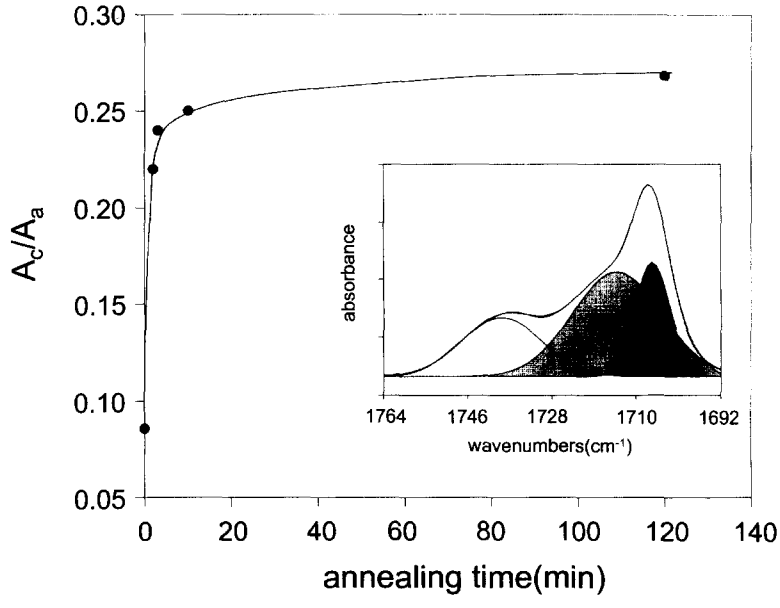

Figure 9 Integrated intensity (C=O in crystal/amorphous) of PBT (PBT/PAr (4/6)) as a function of annealing time. Ac, crystalline C=O peak area; Aa, amorphous C=O peak area of PBT

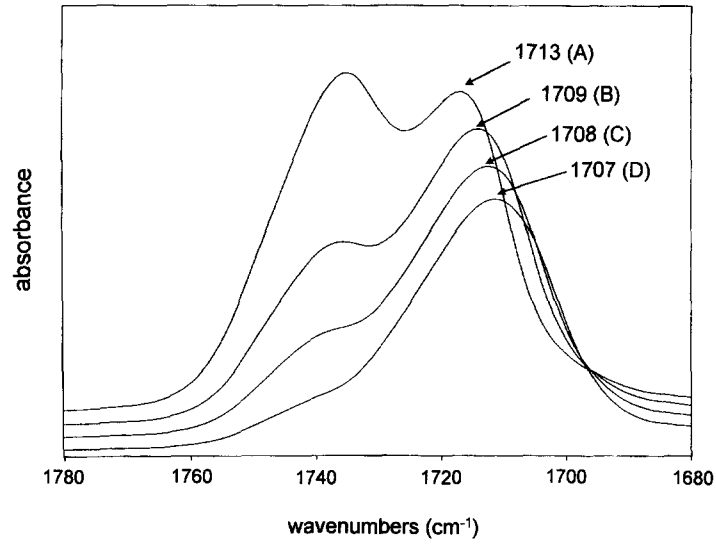

Figure 10 *FT*-i.r. ATR spectra of PBT/PAr blends (annealed for 3 min): (*A*) PBT/PAr (2/8); (*B*) 4/6; (*C*) 6/4; (*D*) 8/2

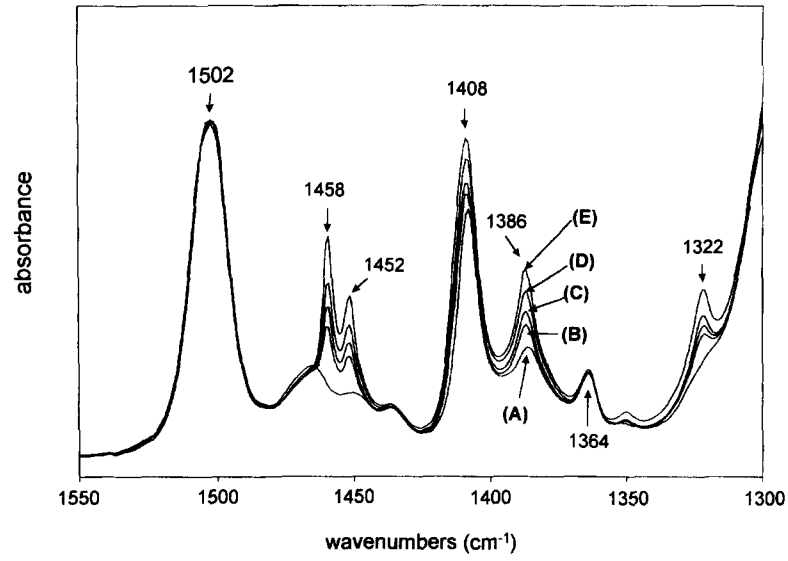

Figure 11 *FT*-i.r. ATR spectra of PBT/PAr (4/6) blend in methylene bending region annealing time: (*A*) 0; (*B*) 2; (*C*) 3; (*D*) 10; (*E*) 120 min

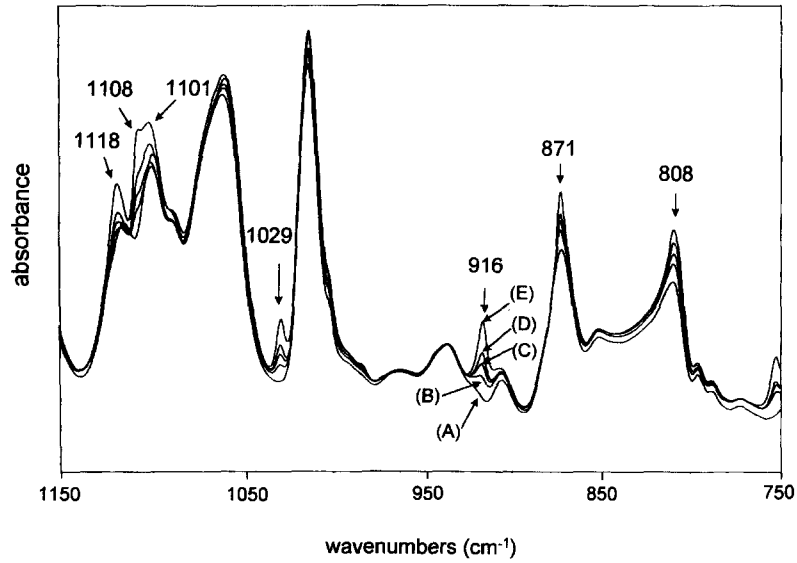

Figure 12 *FT*-i.r. ATR spectra of PBT/PAr (4/6) blend in methylene rocking region annealing time: (*A*) 0; (*B*) 2; (*C*) 3; (*D*) 10; (*E*) 120 min

of PBT/PAr blends. Similar to PBT homopolymer, the characteristic peaks of α crystallinity in PBT are also shown in *Figure 11*. The peaks at 1458 and 1452 cm^{-1} appeared simultaneously and increased with increasing the annealing time. In the case of PBT homopolymer, these peaks were split from the peak at 1455 cm^{-1} on cooling but the peak at 1455 cm^{-1} was not observed in ATR spectra. Other characteristic peaks representing α crystallinity of PBT have a tendency to increase their intensities on annealing. The aromatic ring C–H vibration peak at 1408 cm^{-1} in PBT or PAr slightly increased due to the chain packing effect.

Finally, the methylene rocking region of the same spectra of the PBT/PAr (4/6) blend in the previous figure is shown in *Figure 12*. The peak at 916 cm^{-1} was assigned to the α crystalline phase of PBT. This peak was greatly enhanced as annealing time increased. The aromatic ring C–H vibration in the plane bend is attributed to the peak at 1118 cm^{-1}, and the C–O stretch peak at 1108 and 1101 cm^{-1} also increased with annealing or crystallisation. In the PBT/PAr blend, conformational sensitive bands have a major role in the crystallisation of PBT. For example, the peaks at 1029, 871 and 808 cm^{-1} are conformationally sensitive bands of glycol residues of PBT. There was no characteristic peak representing β crystallinity of PBT[11].

In the PBT/PAr binary blend, the amorphous phase separation has been studied using dynamic mechanical thermal analysis. DMTA thermogram for PBT/PAr (4/6) is shown in *Figure 13*. As the PBT/PAr blend is a completely miscible polymer pair in amorphous or melt state, single transition temperature was observed in 'as-prepared' film. On annealing, a new transition peak was created as a shoulder at a lower temperature. This may be a crystal–amorphous interphase between the PBT crystal phase and the amorphous mixture[1,2]. This new amorphous phase must be a PBT-rich phase judging from its glass transition temperature. In addition, the glass transition temperature of the bulk amorphous phase slightly shifts to a higher temperature. It can be explained that the T_g of the amorphous mixture became higher as PBT crystallised and the portion of PBT in the amorphous phase decreased. In the PBT/PAr (4/6) blend, amorphous phase separation induced by crystallisation of PBT occurred.

On the other hand, as shown in *Figure 14*, some different phase behaviours are observed in PBT/PAr (6/4) blends. As PBT in the PBT/PAr blend crystallised, the T_g of the amorphous mixture became higher for the same reason as the PBT/PAr (4/6) blend system in *Figure 13*. However, a new glass transition peak appeared at higher temperature as a shoulder. This peak was attributed to a PAr-rich phase rejected from the crystalline phase of PBT. From these results, it can be concluded that amorphous phase separation of the PBT/PAr blend at a high weight fraction of PBT is caused by PAr rejected from the crystalline phase of PBT, while the inhomogeneity of the amorphous phase in the PBT/PAr blend at a high weight fraction of PAr is due to the formation of the crystalline–amorphous interphase around the crystalline phase of PBT.

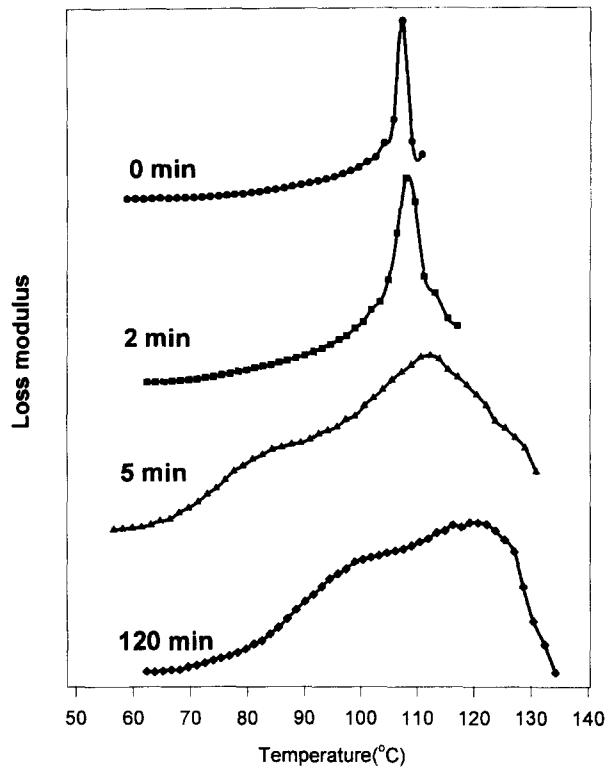

Figure 13 DMTA thermograms of PBT/PAr blend (4/6) as a function of annealing time

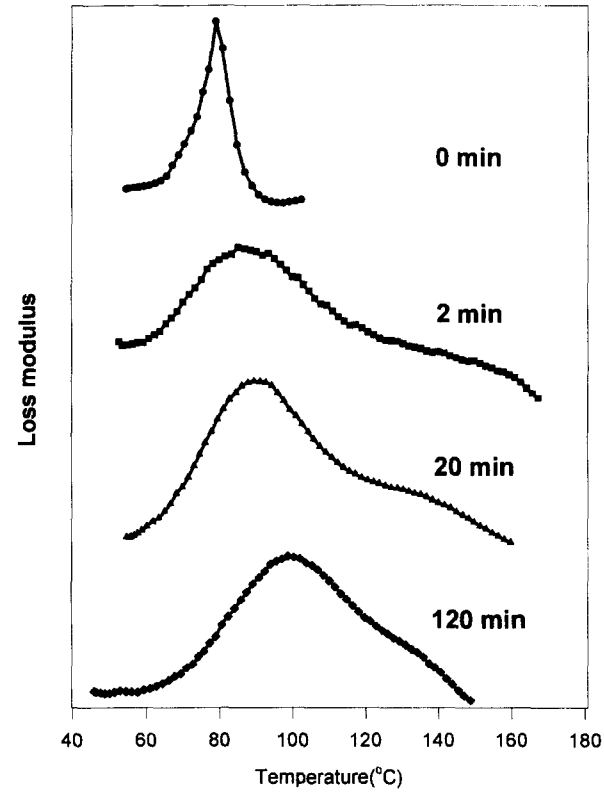

Figure 14 DMTA thermograms of PBT/PAr blend (6/4) as a function of annealing time

CONCLUSION

The crystallisation behaviour of PBT homopolymer and PBT in a PBT/PAr blend was studied using *FT*-i.r. spectrometry, and the phase separation behaviour of the PBT/PAr blend was investigated with a dynamic mechanical analyser. As PBT crystallises, the intensity of the carbonyl stretch band in PBT increases and its frequency shifts to a lower wavenumber.

The characterisation of this frequency and intensity difference was performed by numerical deconvolution and

curve fitting. The higher wavenumber peak was defined as the C=O stretching band of amorphous PBT and the lower wavenumber band as that of crystalline PBT. The relative intensity of the C=O band at the lower wavenumber increased on annealing. Similar behaviour was observed in PBT homopolymer and PBT in the PBT/PAr blend. However, the crystallisation rate of PBT in the PBT/PAr blend is much slower than that of PBT homopolymer due to PAr in blend.

In the *FT*-i.r. spectrum, the C–H rocking mode at 916 cm^{-1} was another useful indicator of crystallinity of PBT in the PBT/PAr blend.

PBT and PAr were completely miscible in the amorphous phase at all compositions. However, phase separation of the amorphous phase occurred with increasing the annealing time, due to crystallisation of PBT in the PBT/PAr blend. In the case of a PBT-rich composition (6/4), phase separation was caused by the rejected PAr from the crystalline phase of PBT. On the contrary, the crystalline–amorphous interphase was formed in the case of PAr-rich compositions (4/6), and amorphous phase separation occurred with the formation of the crystalline–amorphous interphase around the crystalline phase of PBT.

REFERENCES

1. Runt, J., Barron, C. A., Zhang, X. and Kumar, S. K., *Macromolecules*, 1991, **24**, 3466.
2. Runt, J., Zhang, X., Miley, D. M. and Gallargher, K. P., *Macromolecules*, 1992, **25**, 3902.
3. Runt, J., Zhang, X., Miley, D. M., Gallargher, K. P., McFeaters, K. and Fishburn, J., *Macromolecules*, 1992, **25**, 1929.
4. Runt, J., Miley, D. M., Gallargher, K. P., Zhang, X., Barron, C. A. and Kumar, S. K., *Polym. Adv. Tech.*, 1994, **5**, 333.
5. Huo, P. P. and Cabe, P., *Macromolecules*, 1993, **26**, 4275.
6. Huo, P. P. and Cabe, P., *Macromolecules*, 1993, **26**, 5561.
7. Hall, I. H. and Pass, M. G., *Polymer*, 1976, **17**, 807.
8. Brereton, M. G., Davies, G. R., Jakeways, R., Smith, T. and Ward, I. M., *Polymer*, 1978, **19**, 17.
9. Tashiro, K., Nakai, Y., Kobayashi, M. and Tadokoro, H., *Macromolecules*, 1980, **13**, 137.
10. Ward, I. M. and Wilding, M. A., *Polymer*, 1977, **18**, 327.
11. Stambaugh, B., Lando, J. B. and Koenig, J. L., *J. Polym. Sci. Polym. Phys. Ed.*, 1979, **17**, 1063.
12. Siesler, H. W., *J. Polym. Sci. Polym. Lett. Ed.*, 1979, **17**, 453.
13. Gillette, P. C., Lando, J. B. and Koenig, J. L., *Polymer*, 1985, **26**, 235.
14. Kumar, S. K. and Yoon, D. Y., *Macromolecules*, 1989, **22**, 4098.
15. Kimura, M., Porter, P. S. and Salee, G., *J. Polym. Sci. Polym. Phys. Ed.*, 1983, **21**, 367.
16. Miley, D. M. and Runt, J., *Polymer*, 1992, **33**, 4643.
17. Espinosa, E., Maria, J. and Valero, M., *Polymer*, 1993, **34**, 382.
18. Koenig, J. L., *Chemical Microstructure of Polymer Chain*. John Wiley & Sons, New York, 1976.
19. Gillette, P. C., Dirlikov, J. L., Koenig, J. L. and Lando, J. B., *Polymer*, 1982, **23**, 1759.
20. Mark, J. E., *Physical Properties of Polymers Handbook*. AIP Press, New York, 1996.
21. Stein, R. S. and Misra, A., *J. Polym. Sci. Polym. Phys. Ed.*, 1980, **18**, 327.
22. Stambaugh, B., Koenig, J. L. and Lando, J. B., *J. Polym. Sci. Polym. Phys. Ed.*, 1979, **17**, 1053.
23. Mencik, Z., *J. Polym. Sci. Polym. Phys. Ed.*, 1975, **13**, 1975.
24. Eguiazabal, J. I., Val, J. J., Cortazar, M. and Iruin, J. J., *Eur. Polym. J.*, 1991, **27**, 965.
25. Paul, D. R. and Barlow, J. W., *Am. Chem. Soc.*, 1979, **40**, 746.